Quantitative FISH Image Analysis for Telomere Length Measurements

Mark A. Schulze[a], Todd A. Guillory[a], Kenneth R. Castleman[a], Asha S. Multani[b], and Sen Pathak[b]

[a]Perceptive Scientific Instruments, Inc., League City, Texas, U.S.A.
[b]University of Texas M. D. Anderson Cancer Center, Houston, Texas, U.S.A.

Abstract. Quantifying the amount of a specific DNA sequence in a specimen is increasingly important in cytogenetics laboratories. We have developed image analysis tools to measure the length of telomeric DNA repeat sequences using fluorescence microscopy. These tools are useful for the clinical diagnosis of cancer, for finding small chromosome deletions, and for gene expression studies. We will present data that show that specimens with different telomere lengths can be easily distinguished using quantitative FISH analysis, and furthermore that the length differences can be accurately quantified.

1. Introduction

Quantifying the amount of a specific DNA sequence in a specimen is increasingly important in cytogenetics laboratories as genetics research reveals more detailed information about the human genome and gene expression. Cytogeneticists both in clinical practice and in cancer research are increasingly interested in quantitative information about the presence or absence of specific DNA sequences in their specimens. One area of growing interest is in quantifying the amount of telomeric DNA in cancer specimens, since telomeres are important to the stability and replication of chromosomes [1, 2]. Telomere length is of particular importance to cancer researchers, since telomeres are thought to play an important role in senescence and apoptosis [3]. Cancer cells that have long telomeres are postulated to be more likely to metastasise than cancer cells that do not [4-6]. With the introduction of image analysis tools to perform telomere length measurements inexpensively, quickly, and easily, clinical diagnosis of cancer could be significantly improved. These tools will also be useful for finding small chromosome deletions that presently escape detection using FISH techniques, and performing gene expression studies, such as those involving the HER-2/neu gene for breast cancer.

2. Background

In humans, the telomeres consist of a large number (on average, 2000) of $(T_2AG_3)_n$ repeats which are found at the ends of the chromosomes. Since the DNA polymerases that replicate DNA cannot copy chromosomes all the way to the very end, the number of telomeric repeats typically decreases with the number of cell divisions and with age [7]. When chromosomes no longer have any telomeric DNA left at their ends, they tend to "stick together" at the ends, resulting in complex multicentric or ring configurations [1, 8]. Such configurations undergo breakage-fusion-bridge cycles during subsequent cell divisions, usually resulting in cell death [9]. Telomeres are lengthened by the enzyme telomerase, and high levels of telomerase are found in many, but not all, immortal cancer cell lines [10-14].

In cancer cytogenetics, studies of the lengths of telomeres have become increasingly important since cancer cell lines that are not able to maintain telomere length eventually die out. Telomerase mediates this lengthening in many cases, but in some cell lines another mechanism known as ALT (for "Alternative Lengthening of Telomeres") is postulated to be at work [11, 15-17]. In light of these findings, much cancer research will be directed at finding effective methods to block both telomerase and ALT from acting in cancer cells. An accurate, efficient way to measure telomere length will therefore greatly aid cancer researchers.

The brightness of a FISH spot in a microscope image is proportional to the number of fluor molecules present. There are a fixed number of fluor molecules per nucleotide in the DNA probe, and the nucleotides hybridise proportionally to the chromosomal DNA. Thus, except for non-uniform hybridisation and photobleaching effects, the spot brightness is proportional to the amount of the target DNA sequence present. We will present data that show that specimens with different telomere lengths can be easily distinguished using quantitative FISH analysis, and furthermore that the length differences can be accurately quantified.

3. Methodology

Our approach is to use digital image analysis methods to obtain accurate total fluorescence measurements for FISH-labeled structures. When the acquired images have significant background intensity, we use surface fitting and background subtraction for image flattening. Colour compensation [18, 19] is also used to prepare the images for analysis when the fluorescent dyes used have significant emission spectrum overlap. After the images are prepared, the integrated fluorescence brightness is computed for each labelled structure of interest.

We have developed software tools to simplify the process of taking telomere length measurements from fluorescence microscopy images. First, the counterstain image is thresholded, and the resulting objects are found automatically and outlined. Any touching cells are separated manually, and cells that are not completely in the field of view are deselected. The program automatically numbers the objects for analysis. This is illustrated in Figure 1 below. When the cells are segmented to the user's satisfaction, measurements are taken automatically by the program and displayed in a results box, as shown in Figure 2 below.

4. Results

An example of telomere length measurement from fluorescence microscope image analysis is given in Figure 3 below. The specimen shown in Figure 3(***b***) and (***d***) is shown to have significantly more telomeric DNA than the specimen in Figure 3(***a***) and (***c***). Measurements of 48 cells from the cell line shown on the left in Figure 3 were taken, and measurements from 68 cells from the cell line shown on the right of Figure 3 were taken. The resulting measurements were shown to have an acceptable goodness of fit according to the maximum likelihood criterion for the Laplace (double-exponential) distribution. Other distributions did not satisfy the goodness of fit criterion as well as the Laplace distribution. The means of the two distributions were 25 and 37, indicating that the second cell line has approximately 50% more telomeric DNA than the first cell line.

Future work will confirm these results using Southern analysis to verify the average telomere length for cell lines, and will extend this analysis to metaphase chromosomes to show variations in telomere length among chromosomes within a cell. Similar studies have been performed in the laboratories of P. Lansdorp [20-23] and A. Raap and H. Tanke [24].

5. Conclusions

We have illustrated the use of digital fluorescence microscopy to measure fluorescence from probes labelled to repetitive DNA sequences to quantify the relative amount of telomeric DNA present between cell lines. We plan to extend this work to allow the number of $(T_2AG_3)_n$ repeats to be estimated accurately using fluorescence microscopy.

Acknowledgements

This work was supported by a Small Business Innovation Research grant from the United States National Cancer Institute (1 R43 CA82049-01). The authors would also like to thank Kirsten Vang Nielsen of Dako for providing telomere PNA FISH kits for this research.

References

1. S. Pathak, Z. Wang, M. K. Dhaliwal***, et al.***, "Telomeric association: another characteristic of cancer chromosomes?," ***Cytogenetics and Cell Genetics***, vol. 47, pp. 227-229, 1988.
2. V. A. Zakian, "Telomeres: Beginning to understand the end," ***Science***, vol. 270, pp. 1601-1607, 1995.
3. S. Pathak, B. J. Dave, and S. Gagos, "Chromosome alterations in cancer development and apoptosis," ***In Vivo***, vol. 8, pp. 843-850, 1994.
4. T. Takada, T. Hayashi, M. Arakawa***, et al.***, "Telomere elongation frequently observed during tumor metastasis," ***Japanese Journal of Cancer Research***, vol. 82, pp. 1124-1127, 1992.
5. P. N? rnberg, G. Thiel, F. Weber***, et al.***, "Changes of telomere lengths in human intracranial tumours," ***Human Genetics***, vol. 91, pp. 190-192, 1993.
6. Y. Shirotani, K. Hiyama, S. Ishioka***, et al.***, "Alteration in length of telomeric repeats in lung cancer," ***Lung Cancer***, vol. 11, pp. 29-41, 1994.
7. J. Lindsey, N. I. McGill, L. A. Lindsey***, et al.***, "In vivo loss of telomeric repeats with age in humans," ***Mutation Research***, vol. 256, pp. 45-48, 1991.

8. T. K. Pandita, S. Pathak, and C. R. Geard, "Chromosome end associatons, telomeres and telomerase activity in ataxia telangiectasia cells," ***Cytogenetics and Cell Genetics***, vol. 71, pp. 86-93, 1995.
9. S. Pathak, "Centromere of telomere: who is the boss?,"***Anticancer Research***, vol. 15, pp. 2549-2550, 1995.
10. C. W. Greider, "Telomere length regulation,"***Annual Review of Biochemistry*** vol. 65, pp. 337-365, 1996.
11. C. W. Grieder and E. H. Blackburn, "Telomeres, telomerase and cancer," ***Scientific American***, vol. 274, pp. 92-97, 1996.
12. E. Finkel, "Telomeres: keys to senescence and cancer,"***Lancet***, vol. 351, pp. 1186, 1998.
13. Y. Kageyama, S. Kamata, J. Yonese***, et al.***, "Telomere length and telomerase activity in bladder and prostate cancer cell lines," ***International Journal of Urology*** vol. 4, pp. 407-410, 1997.
14. F. Ishikawa, "Telomere crisis, the driving force in cancer cell evolution," ***Biochemical and Biophysical Research Communications***, vol. 230, pp. 1-6, 1997.
15. T. M. Bryan, A. Englezou, L. Dalla-Pozza***, et al.***, "Evidence for an alternative mechanism for maintaining telomere length in human tumors and tumor-derived cell lines," ***Nature Medicine***, vol. 3, pp. 1271-1274, 1997.
16. R. Reddel, T. Bryan, and J. Murnane, "Immortalized cells with no detectable telomerase activity. A review," ***Biochemistry (Moscow)***, vol. 62, pp. 1254-1262, 1997.
17. M. A. Blasco, H. W. Lee, M. P. Hande***, et al.***, "Telomere shortening and tumor formation by mouse cells lacking telomerase RNA," ***Cell***, vol. 91, pp. 25-34, 1997.
18. K. R. Castleman, "Color compensation for digitized FISH images,"***Bioimaging***, vol. 1, pp. 159-165, 1993.
19. K. R. Castleman, "Digital image color compensation with unequal integration periods,"***Bioimaging***, vol. 2, pp. 160-162, 1994.
20. S. S. S. Poon, U. W. Martens, R. K. Ward***, et al.***, "Telomere length measurements using digital fluorescence microscopy," ***Cytometry***, vol. 36, pp. 267-278, 1999.
21. U. M. Martens, M. J. M. Zijlmans, S. S. S. Poon***, et al.***, "Short telomeres on human chromosome 17p," ***Nature Genetics***, vol. 18, pp. 76-80, 1998.
22. N. Rufer, W. Dragowska, G. Thornbury***, et al.***, "Telomere length dynamics in human lymphocyte subpopulations measured by flow cytometry," ***Nature Biotechnology***, vol. 16, pp. 743-747, 1998.
23. P. M. Lansdorp, N. P. Vewwoerd, F. M. van de Rijke***, et al.***, "Heterogeneity in telomere length of human chromosomes," ***Human Molecular Genetics***, vol. 5, pp. 685-691, 1996.
24. E. S. D. De Pauw, N. P. Verwoerd, N. Duinkerken***, et al.***, "Assessment of telomere length in hematopoietic interphase cells using in situ hybridization and digital fluorescence microscopy," ***Cytometry***, vol. 32, pp. 163-169, 1998.

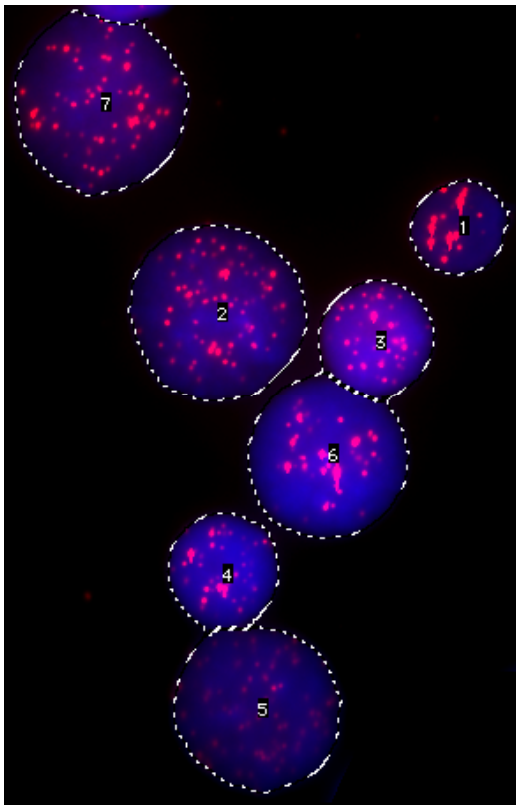

Figure 1. Segmentation of cells in fluorescence microscope image.

Results Window

telomere2 HB1720Q1

Obj#	Area	Mean	Std Dev	Min	Max	Mode	Integrated_Intensity	Red Density
1	2366	44	16.65	26	112	40	104608	62.16
2	8029	45	11.90	26	116	48	367415	55.45
3	3524	60	16.91	26	132	73	212315	71.13
4	3406	51	15.26	25	129	61	176710	52.16
5	7064	37	5.98	23	77	41	265232	40.85
6	6676	52	16.47	24	135	60	351513	53.79
7	7923	43	11.39	26	117	48	346468	58.18

Figure 2. Window displaying results of measurements on objects in Figure 1.

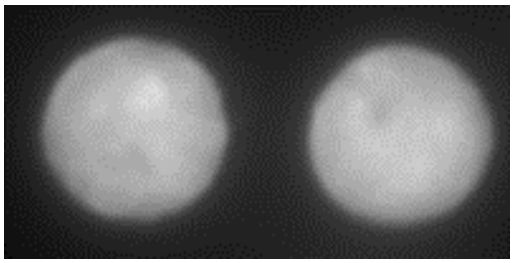

(***a***) DAPI (blue) channel

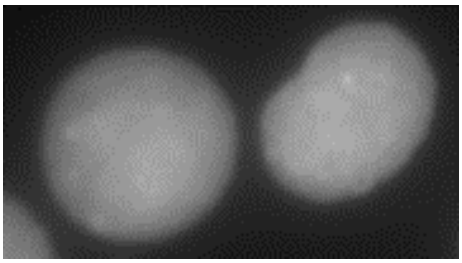

(***b***) DAPI (blue) channel

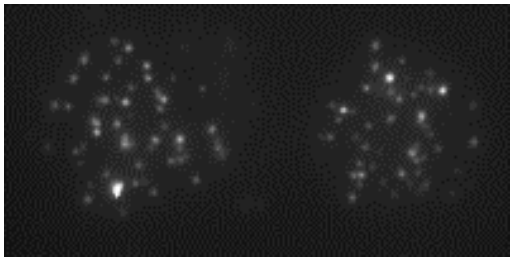

(***c***) Cy3 (red) channel

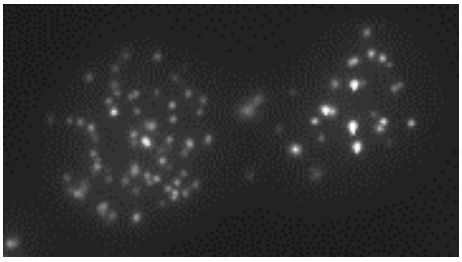

(***d***) Cy3 (red) channel

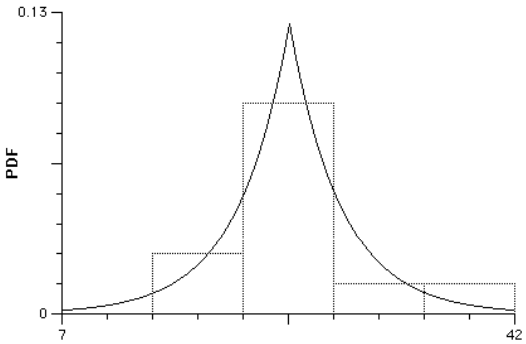

(***e***) θ = 25

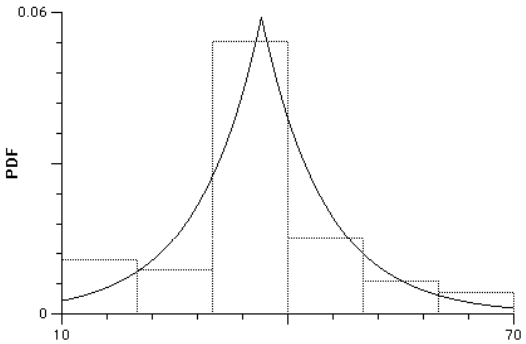

(***f***) θ = 37

Figure 3. (***a***—***d***) Images of interphase nuclei of two different types of prostate cancer cells in blood culture with telomeric DNA labeled with Cy3 (red): (***a***) and (***b***) DAPI counterstain (blue) channel images, and (***c***) and (***d***) Cy3 (red) channel images; (***e***) and (***f***) Histogram of the measurements from 48 cells as in (***c***) and 68 cells as in (***d***) and plots of the maximum-likelihood fitted Laplace (double-exponential) probability density functions.